

# Nanoscale

Accepted Manuscript



This is an *Accepted Manuscript*, which has been through the Royal Society of Chemistry peer review process and has been accepted for publication.

*Accepted Manuscripts* are published online shortly after acceptance, before technical editing, formatting and proof reading. Using this free service, authors can make their results available to the community, in citable form, before we publish the edited article. We will replace this *Accepted Manuscript* with the edited and formatted *Advance Article* as soon as it is available.

You can find more information about *Accepted Manuscripts* in the [Information for Authors](#).

Please note that technical editing may introduce minor changes to the text and/or graphics, which may alter content. The journal's standard [Terms & Conditions](#) and the [Ethical guidelines](#) still apply. In no event shall the Royal Society of Chemistry be held responsible for any errors or omissions in this *Accepted Manuscript* or any consequences arising from the use of any information it contains.

## What Are Grain Boundary Structures in Graphene?

Zheng-Lu Li,<sup>\*†</sup> Zhi-Ming Li,<sup>\*</sup> Hai-Yuan Cao, Ji-Hui Yang, Qiang Shu, Yue-Yu Zhang, H. J. Xiang,<sup>§</sup>  
and X. G. Gong<sup>§</sup>

Key Laboratory of Computational Physical Sciences (Ministry of Education), State Key Laboratory of Surface Physics, and Department of Physics, Fudan University, Shanghai 200433, P. R. China

---

**ABSTRACT:** We have developed a new global optimization method for the determination of interface structure based on the differential evolution algorithm. Here, we applied this method to search for the ground state atomic structures of the grain boundary (GB) between the armchair and zigzag oriented graphene. We find two new grain boundary structures with considerably lower formation energy of about  $1 \text{ eV nm}^{-1}$  than those of the previously widely used structural models. We also systematically investigate the symmetric GBs with GB angle ranging from  $0^\circ$  to  $60^\circ$ , and find some new GB structures. Surprisingly, for intermediate GB angle the formation energy does not depend monotonically on the defect concentration. We also discovered an interesting linear relation between the GB density and the GB angle. Our new method provides important novel route for the determination of GB structures and other interface structures, and our comprehensive study on GB structures could provide new structural information and guidelines to this area.

---

## I. INTRODUCTION

Graphene, the two dimensional (2D) material, shows great application potential<sup>1-3</sup> with the advancement in techniques such as chemical vapor deposition that makes the large-scale growth of graphene feasible.<sup>4-9</sup> In practice, however, graphene is always grown with different defects, among which grain boundary (GB) is one of the most frequently formed defects.<sup>10-12</sup> GBs provide numerous novel possibilities in modifying graphene such as tuning the charge distribution<sup>12</sup> and transport property<sup>13</sup>. Therefore, GBs in graphene have been the focus of numerous researches due to their great significance in science and application.<sup>10-15</sup>

Intensive works have been done to study the broad properties of GBs.<sup>13-29</sup> By analyzing the symmetry between the Brillouin zones of two sides, a theory was developed to predict the electronic transport property through GBs,<sup>13</sup> indicating symmetric GBs have zero transport gap, but the asymmetric GBs have finite gaps. Such predictions are confirmed by non-equilibrium Green's function (NEGF) calculations,<sup>13,16</sup> and provide promising potential to regulate the electric transport properties. As a result, some heterojunctions have already been designed using GBs to develop new transport devices.<sup>17,18</sup> The mechanical responses of under tensile stress were studied by molecular dynamics (MD) simulations.<sup>19-22,28</sup> It is found that the strength of graphene with GBs are affected by not only the density of GBs,<sup>19</sup> but also the local structures at GBs.<sup>19,20</sup> Thermal properties were examined by both NEGF<sup>23</sup> and MD<sup>24-25</sup> techniques, indicating the excellent thermal conductivity of GBs.<sup>23</sup>

Structures are the basis of theoretical investigations on materials, so are the GBs in graphene. People have developed some methods to construct GB structures, e.g., Yazyev and Louie<sup>14</sup> used elementary topological defects to build dislocations and GBs in graphene. However, if we extend the 2D single-composition GB to three dimensional (3D) multi-composition compound interfaces, the complexity of constructing structures from elementary defects would exponentially increase. One kind of promising methods to predict complex structures is the global optimization, which has been successfully applied to predict both 2D and 3D crystal structures.<sup>30-39</sup> However, even this method is so powerful, it may still have a lot of difficulties to overcome in predicting the interface structure, which is usually much more complicated than the corresponding bulk systems, largely increasing the complexity of the task. Initial efforts towards interface structure prediction have been undertaken in some precedent work<sup>40,41</sup> using global optimization algorithms.

Among the numerous global optimization algorithms, differential evolution (DE) has been applied to many fields and achieved great successes.<sup>42-46</sup> DE is based on the idea that using the differentials of randomly selected solution candidates to mutate the existing ones and the generated candidates are accepted only if they have improvements (a greedy strategy). DE is strongly believed to have competitive performance in structure searching be-

cause previous studies showed DE outperforms many other algorithms with the tested functions and problems.<sup>42,44,46</sup>

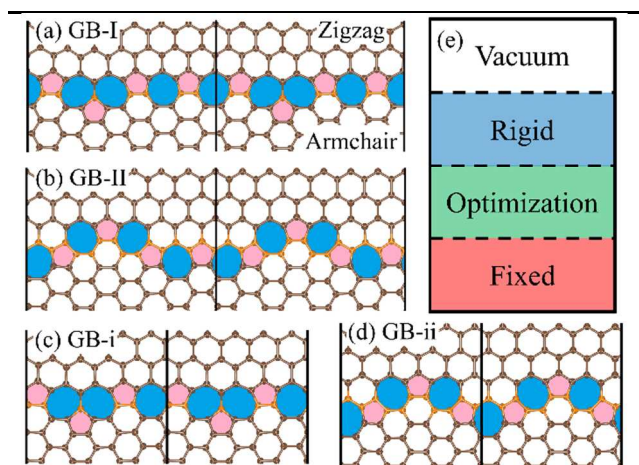


**Figure 1.** (a), (c) The previously widely used structures of GB between armchair and zigzag oriented graphene with the gathering of one pentagon and two heptagons, denoted as (a) GB-I in  $(7, 0)|(4, 4)$  and (c) GB-i in  $(5, 0)|(3, 3)$ . (b), (d) The presently found GB structures with an armchair-like shape, denoted as (b) GB-II in  $(7, 0)|(4, 4)$  and (d) GB-ii in  $(5, 0)|(3, 3)$ . Atoms in the optimization layer are marked using gold color. (e) A schematic illustration of the slab model used in our interface structure prediction.

In this paper, to generally solve the global optimization of the 2D (the GBs in graphene could be viewed as 2D interfaces) and 3D interfaces, we developed a method based on DE algorithm to theoretically predict the interface structures. The performance of our method turns out to be very efficient in searching interface structures, for example, the GBs in graphene, which is the main focus of this work. We first applied our method in one asymmetric case – GB between armchair and zigzag oriented graphene. This type of GB is of great interests<sup>13,15-18,21-25</sup> because people wonder how graphene behaves when the two different types of edges with distinct structural, electronic and magnetic properties meet. It turns out that we have found two new structures [GB-II and GB-ii in Figure 1(b)] with considerably lower formation energy of about  $1 \text{ eV nm}^{-1}$  than the previously widely used one [GB-I in Figure 1(a)]. Then we performed large-scale scan of the symmetric GBs in graphene, with the GB angle varying from  $0^\circ$  to  $60^\circ$ , and we derived the energy curve with respect to GB angle, which is consistent with the previous studies.<sup>14,15,27</sup> We have also found some new GB structures under some specific GB angles that have not been reported before, to our best knowledge. Interestingly, we found that the defect density along the GB direction would be linearly dependent on the GB angle. This relation could be explained by analyzing the specific defect topologies, and could be treated as the guidance in constructing symmetric GB structures in graphene. Our new method

could be generally applied in searching interface structures where broad interesting phenomena emerge. The new structures found in this paper provide different structural basis for the further investigations on GBs in graphene.

## II. METHODS

**DE Based Global Optimization Method for Interface Structure Prediction.** In our approach, we use the slab model to simulate the interface system. As shown in Figure 1(e), we set up the structure with different layers stacking along the  $c$  axis, which is set perpendicular to the  $ab$  plane, and the periodic boundary conditions (PBC) are applied on  $a$  and  $b$  directions. At the bottom is the fixed layer, which means the atoms in this layer is fixed during the whole searching process to simulate the bulk. The optimization layer is in the middle, corresponding to the interfacial region. On the top is the rigid layer, in which the atoms always keep the relative coordinates constant, but could translate as a whole rigid body. During the simulation, besides the degrees of freedom (DOF) of the atomic positions (2 and 3 for the 2D and 3D cases, respectively) in the optimization layer, we also allow three more DOF: the height of the optimization layer and the translation along  $a$  and  $b$  directions for the rigid layer. This operation would lead to more reliable results by avoiding the constraints brought about by the initial setup. The dimension of the problem in the 3D case is thus  $3N_{opt} + 3$ , where  $N_{opt}$  is the number of atoms in the optimization layer.

DE is a global optimization algorithm designed to search the multidimensional continuous spaces to best fit to the designated evaluation functions.<sup>42-46</sup> In the basic DE algorithm, each solution candidate is treated as a vector in the  $D$ -dimensional phase space, and involves in three steps: mutation, crossover and selection. The mutation operation generates a mutant vector  $\mathbf{v}$  for the  $i$ th target vector  $\mathbf{x}$  in the population as follow:

$$\mathbf{v}_{i,G+1} = \mathbf{x}_{r1,G} + F(\mathbf{x}_{r2,G} - \mathbf{x}_{r3,G}) \quad (1)$$

where  $G$  denotes the generation,  $r1$ ,  $r2$  and  $r3$  are random indexes in the population which are mutually different from  $i$ ,  $F$  is a parameter that controls the effect of differential vector. Crossover step creates the trail vector  $\mathbf{u}_{i,G+1} = (u_{1i,G+1}, u_{2i,G+1}, \dots, u_{Di,G+1})$  according to the following scheme:

$$u_{ji,G+1} = \begin{cases} v_{ji,G+1}, & \text{if } r(j) \leq CR \text{ or } j = rn(i) \\ x_{ji,G}, & \text{if } r(j) > CR \text{ and } j \neq rn(i) \end{cases} \quad (2)$$

where  $r(j) \in [0,1]$  is the  $j$ th uniformly generated random number,  $rn(i)$  represents a randomly chosen index of dimension to ensure the  $i$ th target vector gets at least one element from the mutant vector, and  $CR \in [0,1]$  is the crossover probability. Selection in DE simply takes the greedy principle to accept the trail vector only if it is better than the previous corresponding target vector. Two important parameters  $F$  and  $CR$  in DE control the general behaviors of the algorithms and in this work we choose  $F$

= 0.5 and  $CR = 0.9$ . To optimize interface structures using DE, each potential structure corresponds to one target vector with  $D = 3N_{opt} + 3$ .

The use of symmetry constraints<sup>35,36,39</sup> is suggested to significantly improve the performance of global optimization. However, usually the interfacial part has rather low symmetry since the bulk structures on the two sides are always asymmetric. To achieve the high efficiency of global optimization based on DE, we propose another strategy. In DE, operations are applied dimension by dimension. However, it might happen that the vectors corresponding to two interface structures are misaligned, which results in unrealistic high energy structure by the DE operations. Thus, we take a sorting strategy for the atoms in the optimization layer according to their positions, so that structures would not be distorted too much or even destroyed by DE. With this additional sorting step, the efficiency of the global optimization by DE could be kept high.

After all structures are generated by DE in each generation, all the  $3N_{opt} + 3$  DOF of every structure will be relaxed to its local minimum, using either empirical potentials or first-principles calculations. In this work, because of the 2D nature of graphene, the DOF is reduced to  $D = 2N_{opt} + 2$ . The local optimization is a common routine in structure prediction, aiming to effectively reduce the search space and to get total energy of each structure.

**Empirical Potentials Calculations.** Our empirical potentials calculations are performed using LAMMPS<sup>47</sup> with the widely used AIREBO potential<sup>48</sup> for graphene systems. For local optimization in DE searching, we minimize the total energy of every structure using conjugate gradient method. For the molecular dynamics (MD) simulations which are used to get the mechanical property of the structure finally predicted by DE, we use the following method:<sup>20</sup> MD simulations are performed using  $NVE$  ensemble, i.e., atom number, volume and energy are constant, the cutoff radius of C-C bond  $r_{CC}$  is set 1.92 Å, the graphene sheets are applied with uniaxial strain at a rate of  $10^{-9} \text{ s}^{-1}$ , and Virial stresses are calculated (See results on stress in Supporting Information).

**First-principles Calculations.** The first-principles calculations based on DFT are performed using VASP<sup>49</sup> with the projected augmented wave method.<sup>50,51</sup> We use first-principles calculations to ensure the final results from DE and to study the electronic properties. For such purposes, we use the local density approximation to describe the exchange-correlation potential in the DFT calculations. Structures are relaxed until the atomic forces are less than 0.01 eV/Å and total energies are converged to  $10^{-6}$  eV with the cutoff energy for plane-wave basis wave functions set to 400 eV.

**Searching Criterion.** We intend to search the structure of the GB between the armchair and zigzag oriented graphene as an example of illustration.

For this type of GB, many of the abovementioned works<sup>13,15-18,21-25</sup> adopted two similar GB structures shown in Figure 1(a) and (c), denoted as GB-I and GB-i in this

work, corresponding to (7, 0)|(4, 4) and (5, 0)|(3, 3) lattice matching respectively. Both GB-I and GB-II present the same structural character that one pentagon and two heptagons gathered at one point (fly-head pattern). However, the gathering of defects is likely to increase the intrinsic stress,<sup>22</sup> making the structure relatively unstable with high energy, similar to the isolated pentagon rule in determining the structures of fullerenes.<sup>52,53</sup> Thus, a quite serious and questionable issue is whether GB-I or GB-II is the ground state structure of the GB between the armchair and zigzag oriented graphene. Therefore, it is desirable to reinvestigate this GB structure using the method we developed in this work.

Since we use the slab model to simulate the interface structure with one dimensional PBC, the structure we used is actually carbon nanoribbon with GB parallel to the edges. The two edges are passivated by hydrogen atoms, and are about 15 Å away from the GB. For each case of lattice matching, we keep the fixed and rigid layers the same, and perform a series of searching with different numbers of atoms in the optimization layer. We adopt a simple searching criterion to minimize the relative formation energy defined below:

$$\Delta E_{form}(N_{opt}) = [E_{tot}(N_{opt}) - E_{tot}(\text{GB-I}) - (N_{opt} - 7) \times \mu_C] / L \quad (3)$$

where  $\Delta E_{form}$  is the relative formation energy,  $E_{tot}(N_{opt})$  the total energy of the structure with a certain  $N_{opt}$ , and  $\mu_C$  the chemical potential of one carbon atom taken from pristine graphene. In fact, we are using GB-I as the zero point in the comparisons, i.e.,  $\Delta E_{form}(\text{GB-I}) = 0$ , because  $N_{opt} = 7$  for GB-I (see Table 1). This equation is used in searching structures specifically in (7, 0)|(4, 4) GB, with a certain periodicity  $L$  along GB. For (5, 0)|(3, 3) GB, Eq. (3) could be rewritten by substituting GB-II for GB-I and  $(N_{opt} - 5)$  for  $(N_{opt} - 7)$ , because  $N_{opt} = 5$  for GB-II (see Table 1).

To get the absolute graphene GB formation energy so that we could compare different structures in a more direct manner, we construct the periodic structures made of only carbon atoms by applying inversion symmetry to the slabs we used in the global optimization. The absolute formation energy could be written as:<sup>21</sup>

$$E_{form} = (E_{tot} - N \times \mu_C) / 2L \quad (4)$$

where  $E_{tot}$  denotes the total energy of the periodic cell containing two equivalent GBs with the length of GB  $L$ , and  $N$  the total number of atoms in the cell.

### III. RESULTS AND DISCUSSIONS

**Predicting Armchair-Zigzag Grain Boundary Structures.** Our method is quite efficient in finding the lowest-energy structures, and one benchmark is provided in the Supporting Information. For the (7, 0)|(4, 4) GB, we scan a large range of  $N_{opt}$  and plot our results in the upper panel of Figure 2. When  $N_{opt} = 15$ , a new GB structure is found, shown as GB-II in Figure 1(b). After full structural relaxation by DFT, we obtain  $E_{form}(\text{GB-I}) = 4.29 \text{ eV nm}^{-1}$  and

$E_{form}(\text{GB-II}) = 3.22 \text{ eV nm}^{-1}$  (see Table 1), indicating that the formation energy of GB-II is  $1.07 \text{ eV nm}^{-1}$  (a considerably large formation energy difference) lower than GB-I. The reason for this is quite simple. GB-I structure possesses a gathering of one pentagon and two heptagons, while GB-II is just a clean pentagon-heptagon chain with armchair-like shape. Since the gathering of the pentagon and heptagon defects in graphene usually leads to higher energy, GB-II could effectively reduce the formation energy comparing with GB-I. Interestingly, when  $N_{opt} = 14$ , we found a structure [see upper panel of Figure 2] that has slightly lower formation energy than GB-I by empirical potential calculations. This structure has a hole in the GB and actually if one additional carbon atom is added to the middle of the hole, it would become GB-II.

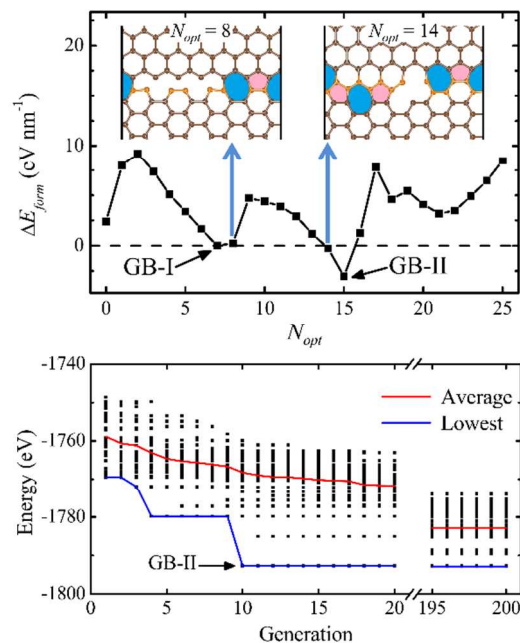


**Figure 2.** The upper panel: the relative formation energy  $\Delta E_{form}$  to GB-I by empirical potential for each  $N_{opt}$ . GB-II structure is found to have the lowest formation energy. Structures with  $N_{opt} = 8$  and  $14$  are shown in insets. The lower panel: performance of our method based on DE algorithm. Black dots represent the total energy evaluated for the structures in each generation. GB-II is found in 10 generations, indicating high efficiency of our method.

We also compute other properties of armchair-zigzag GBs. For instance, we have performed MD simulations, showing that GB-II has a better mechanical property under uniaxial strain. STM image simulations from first-principles calculations show that GB-I and GB-II can be distinguished by the STM technique. (See details and results of MD and STM simulations in Supporting Information)

**Table 1. Formation energies of four GBs.  $N_{opt}$  is the number of atoms in the optimization layer.**

GBs	GB-I	GB-II	GB-i	GB-ii
$N_{opt}$	7	15	5	11
$E_{form}$ (eV nm <sup>-1</sup> )	4.29	3.22	5.45	4.41

For (5, 0)|(3, 3) GB, we also find a new structure GB-ii, which has a considerably lower formation energy of 1.04 eV nm<sup>-1</sup> than GB-i (see Table 1). Actually, GB-I and GB-i are similar, and GB-II is similar to GB-ii as well (see Figure 1): comparing with GB-I, GB-i lacks one pentagon-heptagon pair; if we take one pentagon-heptagon pair away from GB-II, it naturally becomes GB-ii. However, (5, 0)|(3, 3) GB has a larger lattice mismatch than (7, 0)|(4, 4) GB (3.8% to 1.0%). According to Eq. (4), when calculating the absolute formation energy, with two equivalent GBs in one unit cell, the farther the two GBs separate, (5, 0)|(3, 3) GB would have larger formation energy than (7, 0)|(4, 4) GB, because the graphene part between GBs would get higher energy due to the strain effect. To avoid ambiguity, we address here that for all periodic structures in this work, we have two equivalent GBs in one unit cell separated by about 30 Å from each other. Because (7, 0)|(4, 4) GB has a smaller lattice mismatch and lower formation energy (see Table 1), practically it is more preferable experimentally, and we would mainly focus on this type of GB. In all four structures considered in this work, GB-II has the lowest formation energy (see Table 1).

Before further investigation on other GB structures, we first demonstrate the global optimization efficiency of our algorithm for (7, 0)|(4, 4) GB. In our DE simulations, we set the size of population to 30, and the maximum generation number 50. To check the reliability and efficiency of our methods, we have performed ten separate independent DE simulations  $N_{opt} = 15$  and all found GB-II structure. The smallest number of generation of finding GB-II is 4, the largest 23, and the average 12.2, evidencing highly efficient performance in this 32-dimensional optimization problem. The lower panel of Figure 2 shows the history of one typical search for the  $N_{opt} = 15$  case, with the maximum generation number set 200 for the purpose of analysis. In this case, the program finds GB-II in 10 generations. Note that the average energy of all structures keeps decreasing during the simulation owing to the greedy selection, indicating good convergence of our method based on DE.

**Predicting Symmetric Grain Boundary Structures.** Yazyev and Louie<sup>14</sup> showed that usually there are three types of dislocations in graphene GBs, as shown in Figure 3 (a – c). Burgers vector  $\vec{b}_{(n,m)} = n\vec{a}_1 + m\vec{a}_2$  is used to describe the dislocations. In the (1, 0) dislocation, the pentagon-heptagon pair is symmetrically along the GB direction. In the (1, 1) dislocation, the pentagon-heptagon pair

is till along the GB direction, but the pentagon and the heptagon are separated by hexagons. The third type is (1, 0) + (0, 1) dislocation, where there are two pentagon-heptagon pairs, and neither of them is along the GB direction. In this type of dislocation, if the two pentagon-heptagon pairs are adjacent, then it is named as paired type [Figure 3(b)], otherwise it is named as disperse type [see, e.g., Figure S6(f) in Supporting Information]. Besides the above three main dislocations, there is another transition state between the (1, 0) and (1, 0) + (0, 1) dislocation, where both characters exist [see Figure 3(e) for example].

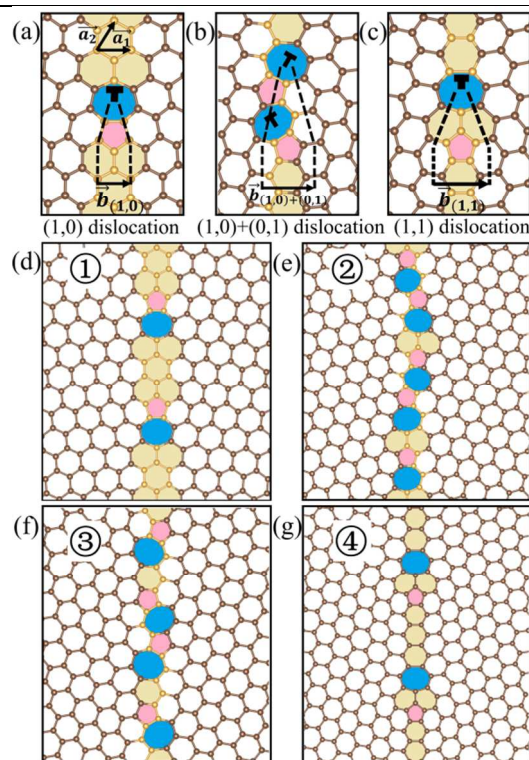


**Figure 3.** (a – c) Three types of dislocations.<sup>14</sup> Listed are the examples for (d) (1, 0) dislocation, (e) transition region, (f) (1, 0) + (0, 1) dislocation and (g) (1, 1) dislocation. (d – g) show one periodicity along the GB direction in each case, and the numbers in the figures correspond to those in Figure 4. In this Figure, (f) and (g) are new structures reported in this work.

We searched quite a few symmetric GBs with the angle ranging from 0° to 60°, and we have successfully found the structures that have been reported before, and some new structures at the angles that has not been reported yet, to our best knowledge.<sup>14,15,27</sup> Also, by the construction principles,<sup>14</sup> i.e., three types of dislocation, we also manually created some GBs with higher energy but reasonable structures. Here are some examples shown in Figure 3(d – g), where Figure 3(f) and (g) are the new structures that have not been reported. (See all structures studied in this work in Supporting Information)

For all the GB structures obtained by DE or manual construction we calculated their absolute formation ener-

gy using empirical potential with Eq. 4. The obtained formation energies with respect to the angle of the symmetric GBs are shown in the upper panel of Figure 4, and all structures are relaxed without 2D restriction, i.e., they are allowed to relax in the third dimension. We find that all the lowest energy structures at each angle can be found by our DE method. The newly found structures in this work are denoted by solid symbols in Figure 4, and those reported before are denoted by empty symbols. From the upper panel of Figure 4, we find that in small angle GBs, (1, 0) dislocation will dominate the structures. However, at large angle GBs, both (1, 0) + (0, 1) and (1, 1) dislocations could be constructed reasonably, but usually, (1, 0) + (0, 1) dislocation would lead to lower formation energy, which is consistent with previous study.<sup>14,27</sup>

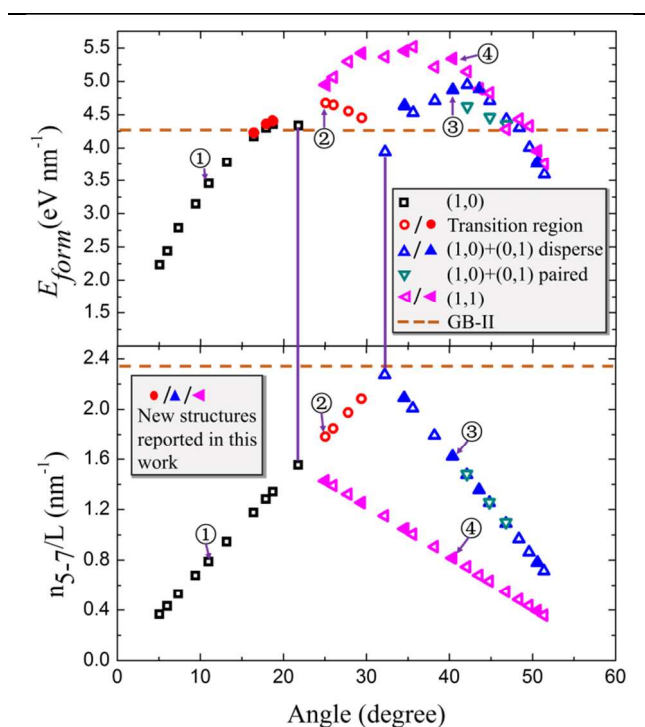


**Figure 4.** Upper panel: Formation energy versus symmetric GB angle. All energies are derived from the empirical potentials calculation, including GB-II, which is used as comparison, after fully relaxation in 3D space, denoted by brown dashed line. Lower panel, dependence of GB density along the GB direction on the GB angle. All detailed structural information of these structures is in Supporting Information. Solid points are the new structures found in this work, while the empty ones are the structures previously proposed.<sup>14,15,27</sup>

Very interestingly, from the lower panel in Figure 4, one can find the number of pentagon-heptagon pair  $n_{5-7}$  per GB length, shows a linear dependence on the GB angle. The slope is uniquely dependent on the type of dislo-

cation in the GB. Generally speaking, the pentagon-heptagon pair  $n_{5-7}$  density not only depends on the grain boundary angle, but also depends on the type of dislocation. For the small GB angles, the defect density linearly increases with the GB angle, while for the large GB angles the defect density linearly decreases with the GB angle. The highest density is observed near  $32.2^\circ$ . Considering the low energy structures, at the small angle side the dislocation type is (1, 0), while the large angle side the dislocation type is (1, 0) + (0, 1). Another special point at  $21.8^\circ$  can be also considered as pseudo-maximum of the defect density, which is a turning point of the dislocation type changing from (1, 0) to (1, 1), although the GBs with dislocation (1, 1) are meta-stable structure. These two points could be treated as the dislocation type transition points, which are corresponding to a local minimum of the formation energy, as shown in Figure 4. In other word, at such points, the GB structures are highly symmetric,<sup>27</sup> the characters of two types of dislocations could coexist, as the strain in bonds are very small at these angle, and thus the formation energy has local minima in terms of GB angle. These linear relations could be proved by analyzing the topological characters of the different types of dislocations.

Generally, the formation energy should have positive correlation with the defect density. However, one can surprisingly see the non-monotonic behavior between defect density and formation energy in Figure 4. Actually, the monotonic behavior appears only for the small angle and large angle side. During the transition region between  $21.8^\circ$  and  $32.2^\circ$ , the strain energies in GB are relaxed, so the formation energies vary only slightly. However, from  $32.2^\circ$  to around  $42.0^\circ$ , although it has only one kind of defect, the formation energy increases with decreasing the defect density. The reason could be that, in this region (greater than  $32.2^\circ$ ), as GB angle increasing, the distance between the pairs of pentagon-heptagon also increases [see structures of (1, 0) + (0, 1) dislocation in Figure S6 in Supporting Information], which decreases the interaction between pentagon-heptagon pairs<sup>29</sup> resulting in a small increase in the formation energy. While the GB angle is larger than around  $42.0^\circ$ , the distance between the pairs becomes large enough, and the interaction between pairs becomes negligible, thus the formation energy of GB decreases with the decrease in the defect density.

In Figure 4, the formation energy and the defect density of armchair-zigzag GB-II is also plotted for comparison, but note that GB-II is asymmetric (with GB angle  $30^\circ$ ) rather than symmetric. What is counterintuitive is that at the highest GB density, e.g., GB-II and the topmost point at  $32.2^\circ$  in lower panel of Figure 4, they have relatively lower formation energies within the neighboring GB angles. This can be understood as follows. In fact, the formation energy is highly dependent on the local distortion of the C-C bonds. These two structures have energetically favorable arrangements of the pentagon-heptagon pairs so that the strain energy is sufficiently released, resulting in lower formation energies.

## IV. CONCLUSION

To predict the structure of interface, we have developed a global optimization method using DE algorithm. We have applied our method to searching the structure of GB between the armchair and zigzag oriented graphene, and found the new structure GB-II (GB-ii) that has a  $1.07 \text{ eV nm}^{-1}$  ( $1.04 \text{ eV nm}^{-1}$ ) lower formation energy than the previously widely used GB-I (GB-i) in (7, 0)|(4, 4) GB [(5, 0)|(3, 3) GB].<sup>54</sup> We have comprehensively studied the symmetric GBs with GB angle ranging from  $0^\circ$  to  $60^\circ$ . We pointed out the linearity between the defects density along the GB direction and the GB angle, however the formation energy does not show monotonic behavior with defect density. The results in this work provide new insight on the structures and properties of GBs in graphene.

**Supporting Information.** Benchmark of our method, properties of armchair-zigzag GB structures, all GB structures studied in this work.

## AUTHOR INFORMATION

### Corresponding Author

§ hxiang@fudan.edu.cn

§ xggong@fudan.edu.cn

\* These two authors contributed equally in this work.

† Present address: Department of Physics, University of California, Berkeley, California 94720, USA

## ACKNOWLEDGMENT

The authors thank M. Ji, X. Gu, S. Chen and Z. Guo for insightful discussions. The work was partially supported by the Special Funds for Major State Basic Research, National Science Foundation of China (NSFC), Program for Professor of Special Appointment (Eastern Scholar), and Foundation for the Author of National Excellent Doctoral Dissertation of China.

## REFERENCES

1. K. S. Novoselov, A. K. Geim, S. V. Morozov, D. Jiang, M. I. Katsnelson, I. V. Grigorieva, S. V. Dubonos and A. A. Firsov, *Nature* 2005, **438**, 197.
2. Y. Zhang, Y.-W. Tan, H. L. Stormer and P. Kim, *Nature* 2005, **438**, 201.
3. A. K. Geim and K. S. Novoselov, *Nature Materials* 2007, **6**, 183.
4. A. Reina, X. Jia, J. Ho, D. Nezich, H. Son, V. Bulovic, M. S. Dresselhaus and J. Kong, *Nano Lett.* 2009, **9**, 30.
5. M. P. Levendorf, C. S. Ruiz-Vargas, S. Garg and J. Park, *Nano Lett.* 2009, **9**, 4479.
6. Q. Yu, J. Lian, S. Siriponglert, H. Li, Y. P. Chen and S.-S. Pei, *App. Phys. Lett.* 2008, **93**, 113103.
7. X. Li, W. Cai, J. An, S. Kim, J. Nah, D. Yang, R. Piner, A. Velamakanni, I. Jung, E. Tutuc, S. K. Banerjee, L. Colombo and R. S. Ruoff, *Science* 2009, **324**, 1312.
8. K. S. Kim, Y. Zhao, H. Jang, S. Y. Lee, J. M. Kim, K. S. Kim, J.-H. Ahn, P. Kim, J.-Y. Choi and B. H. Hong, *Nature* 2009, **457**, 706.
9. Q. Yu, L. A. Jauregui, W. Wu, R. Colby, J. Tian, Z. Su, H. Cao, Z. Liu, D. Pandey, D. Wei, T. F. Chung, P. Peng, N. P. Guisinger, E. A. Stach, J. Bao, S.-S. Pei and Y. P. Chen, *Nature Materials* 2011, **10**, 443.
10. P. Y. Huang, C. S. Ruiz-Vargas, A. M. van der Zande, W. S. Whitney, M. P. Levendorf, J. W. Kevek, S. Garg, J. S. Alden, C. J. Hustedt, Y. Zhu, J. Park, P. L. McEuen and D. A. Muller, *Nature* 2011, **469**, 389.
11. D. L. Duong, G. H. Han, S. M. Lee, F. Gunes, E. S. Kim, S. T. Kim, H. Kim, Q. H. Ta, K. P. So, S. J. Yoon, S. J. Chae, Y. W. Jo, M. H. Park, S. H. Chae, S. C. Lim, J. Y. Choi and Y. H. Lee, *Nature* 2012, **490**, 235.
12. J. Lahiri, Y. Lin, P. Bozkurt, I. I. Oleynik and M. Batzill, *Nature Nanotechnology* 2010, **5**, 326.
13. O. V. Yazyev and S. G. Louie, *Nature Materials* 2010, **9**, 806.
14. O. V. Yazyev and S. G. Louie, *Phys. Rev. B* 2010, **81**, 195420.
15. Y. Liu and B. I. Yakobson, *Nano Lett.* 2010, **10**, 2178.
16. J. Zhang, J. Gao, L. Liu and J. Zhao, *J. App. Phys.* 2012, **112**, 053713.
17. X.-F. Li, L.-L. Wang, K.-Q. Chen and Y. Luo, *J. Phys. Chem. C* 2011, **115**, 12616.
18. X.-F. Li, L.-L. Wang, K.-Q. Chen and Y. Luo, *J. Phys.: Condens. Matter* 2012, **24**, 095801.
19. R. Grantab, V. B. Shenoy and R. S. Ruoff, *Science* 2010, **330**, 946.
20. Y. Wei, J. Wu, H. Yin, X. Shi, R. Yang and M. Dresselhaus, *Nature Materials* 2012, **11**, 759.
21. J. Zhang, J. Zhao and J. Lu, *ACS Nano* 2012, **6**, 2704.
22. B. Wang, Y. Puzyrev and S. T. Pantelides, *Carbon* 2011, **49**, 3983.
23. Y. Lu and J. Guo, *App. Phys. Lett.* 2011, **101**, 043112.
24. H.-Y. Cao, H. Xiang and X.-G. Gong, *Solid State Comm.* 2012, **152**, 1807.
25. A. Bagri, S.-P. Kim, R. S. Ruoff and V. B. Shenoy, *Nano Lett.* 2011, **11**, 3917.
26. J. Zhou, T. Hu, J. Dong and Y. Kawazoe, *Phys. Rev. B* 2012, **86**, 035434.
27. T.-H. Liu, G. Gajewski, C. W. Pao and C.-C. Chang, *Carbon* 2011, **49**, 2306.
28. Z. Song, V. I. Artyukhov, B. I. Yakobson and Z. Xu, *Nano Lett.* 2013, **13**, 1829.
29. J. M. Carlsson, L. M. Ghiringhelli and A. Fasolino, *Phys. Rev. B* 2011, **84**, 165423.
30. C. W. Glass, A. R. Oganov and N. Hansen, *Computer Phys. Comm.* 2006, **175**, 713.
31. G. Trimarchi and A. Zunger, *Phys. Rev. B* 2007, **75**, 104113.
32. M. Ji, K. Umamoto, C.-Z. Wang, K.-M. Ho and R. M. Wentzcovitch, *Phys. Rev. B* 2011, **84**, 220105(R).
33. D. J. Wales and J. P. K. Doye, *J. Phys. Chem. A* 1997, **101**, 5111.

34. A. Nayeem, J. Vila and H. A. Scheraga, *J. Computer Chem.* 1991, **12**, 594.
35. Y. Wang, J. Lv, L. Zhu and Y. Ma, *Phys. Rev. B* 2010, **82**, 094116.
36. Y. Wang, J. Lv, L. Zhu and Y. Ma, *Computer Phys. Comm.* 2012, **183**, 2063.
37. X. Luo, J. Yang, H. Liu, X. Wu, Y. Wang, Y. Ma, S.-H. Wei, X. Gong and H. Xiang, *J. Am. Chem. Soc.* 2011, **133**, 16285.
38. C. J. Pickard and R. J. Needs, *Phys. Rev. Lett.* 2006, **97**, 045504.
39. C. J. Pickard and R. J. Needs, *J. Phys.: Condens. Matter* 2011, **23**, 053201.
40. A. L.-S. Chua, N. A. Benedek, L. Chen, M. W. Finnis and A. P. Sutton, *Nature Materials* 2010, **9**, 418.
41. H. J. Xiang, J. L. F. Da Silva, H. M. Branz and S.-H. Wei, *Phys. Rev. Lett.* 2009, **103**, 116101.
42. R. Storn and K. J. Price, *Global Optimization* 1997, **11**, 341.
43. R. Storn, *Biennial Conference of the North American Fuzzy Information Processing Society (NAFIPS)* 1996, pp. 519–523.
44. K. V. Price, *Biennial Conference of the North American Fuzzy Information Processing Society (NAFIPS)* 1996, pp. 524–527.
45. K. Price, R. M. Storn and J. A. Lampinen, *Differential Evolution: A Practical Approach to Global Optimization*, Springer 2005, ISBN 978-3-540-20950-8.
46. Z. Chen, X. Jiang, J. Li, S. Li and L. Wang, *J. Comp. Chem.* 2013, **34**, 1046.
47. S. Plimpton, *J. Comp. Phys.* 1995, **117**, 1.
48. S. J. Stuart, A. B. Tutein and J. A. Harrison, *J. Chem. Phys.* **b**, **112**, 6472.
49. G. Kresse and J. Furthmüller, *Phys. Rev. B* 1996, **54**, 11169.
50. P. E. Blöchl, *Phys. Rev. B* 1994, **50**, 17953.
51. G. Kresse, D. Joubert, *Phys. Rev. B* 1999, **59**, 1758.
52. H. W. Kroto, K. McKay, *Nature* 1988, **331**, 328.
53. T. G. Schmalz, W. A. Seitz, D. J. Klein and G. E. Hite, *J. Am. Chem. Soc.* 1988, **110**, 1113.
54. The GB structures observed experimentally are sometimes not global minimum in formation energy due to some other factors (such as entropy or non-equilibrium growth). In most cases, our strategy for finding the lowest formation energy should provide clues to the detailed GB structures. If the readers are interested in experimental results, they could refer to the above mentioned references and also the following references: B. I. Yakobson and F. Ding, *ACS Nano* 2011, **5**, 1569; P. Nemes-Incze, P. Vancsó, Z. Osváth, G. I. Márk, X. Jin, Y.-S. Kim, C. Hwang, P. Lambin, C. Chapelier and L. PéterBiró, *Carbon* 2013, **64**, 178.